Invertebrate Biology

Observations on torquaratorid acorn worms (Hemichordata, Enteropneusta) from the North Atlantic with descriptions of a new genus and three new species

Imants G. Priede,[1] Karen J. Osborn,[2] Andrey V. Gebruk,[3] Dan Jones,[4] David Shale,[5] Antonina Rogacheva,[3] and Nicholas D. Holland[6,a]

[1] Oceanlab, University of Aberdeen, Aberdeen AB41 6AA, UK
[2] Department of Invertebrate Zoology, Smithsonian Institution, National Museum of Natural History, Washington, DC 20560, USA
[3] P. P. Shirshov Institute of Oceanology, Russian Academy of Sciences, Moscow 117997, Russia
[4] National Oceanography Centre, Southampton, Hampshire SO14 3ZH, UK
[5] Rosemary Cottage, Rosemary Lane, Musbury, Axminster, Devon EX13 8AS, UK
[6] Division of Marine Biology, Scripps Institution of Oceanography, La Jolla, California 92093-0202, USA

Abstract. Enteropneusts in the family Torquaratoridae were imaged using still and video cameras in the deep North Atlantic and then collected by remotely operated vehicles. From this material, we describe *Yoda purpurata* n. gen, n. sp., *Tergivelum cinnabarinum* n. sp., and *Allapasus isidis* n. sp. Individuals of the first two species were browsing completely exposed on the sea floor, whereas the specimen of the last species was encountered floating ~1 m above the sea floor. Living specimens of *Y. purpurata* were 12–19 cm long and had a dark reddish-purple proboscis, collar, and genital wings (folded dorsally over the anterior region of the trunk). Members of this species were hermaphrodites (the first ever discovered in the phylum Hemichordata), with numerous separate testes and ovaries in the genital wings. Living specimens of *T. cinnabarinum* were 12–26 cm long and had a cinnabar-colored proboscis, collar, and back veils (arising from the anterior region of the trunk); sexes were separate, and body shape and internal morphology closely resemble those of its brown congener, *T. baldwinae*, from the eastern Pacific. The only specimen of *A. isidis* collected was a male 13 cm long and pale yellow when alive. Its body shape was proportionally shorter and broader than that of its orange congener, *T. aurantiacus*, from the eastern Pacific, but the internal anatomy of the two species is virtually identical.

Additional key words: hermaphrodite, Torquaratoridae, benthopelagic lifestyle

Hemichordata is a small phylum of ~140 described extant species, four fifths comprising class Enteropneusta and the rest class Pterobranchia. Enteropneusts, commonly called acorn worms, share some anatomical features with vertebrates, namely pharyngeal gill pores and, more contentiously, a dorsal hollow nerve cord and notochord (=stomochord) (Newell 1952; Hall 2005). Consequently, morphologists have long debated whether enteropneust-like creatures gave rise to the vertebrates (reviewed by Gee 1996). Interest in this phylogenetic scenario has recently been renewed by the discovery of some similarities between the genetic programs that direct the development of acorn worms and

vertebrates (Lowe 2008). As a result, acorn worms continue to attract attention far out of proportion to the modest number of living species in the group.

For over a century, three enteropneust families were recognized (Ptychoderidae Spengel 1893, Spengelidae Willey 1899, and Harrimaniidae Spengel 1902). More recently, a fourth family, the Torquaratoridae Holland et al. 2005, was described. Although this last family was greeted with the criticism that its members probably belonged within the Ptychoderidae (Cannon et al. 2009; Anderson et al. 2011), the validity of the Torquaratoridae was established robustly by the molecular phylogenetic analysis of Osborn et al. (2012), who also re-diagnosed the family on morphological grounds. All torquaratorids observed so far have been on or a short distance above the

[a]Author for correspondence.
   E-mail: nholland@ucsd.edu

deep-sea floor at depths between ~1.6 and 8.8 km (Smith et al. 2005; Osborn et al. 2012). Moreover, most (and possibly all) torquaratorids, in spite of their morphological diversity, are capable of floating in the water column from one benthic foraging site to the next. While deposit feeding, the worms typically crawl slowly, completely exposed on the bottom while leaving behind a more or less continuous trail of feces (a convenient marker of their feeding path). The only known exception is one species that can spend part of the time in shallow burrows (Holland et al. 2012).

Although still and video images have revealed well over a dozen kinds of torquaratorids on the deep-sea floor or floating a short distance above it, relatively few of these worms have been collected, and only three have been formally described. These three, all from the Pacific Ocean, are *Torquarator bullocki* Holland et al. 2005, *Tergivelum baldwinae* Holland et al. 2009, and *Allapasus aurantiacus* Holland et al. 2012. This article concerns three additional torquaratorids, all collected from the deep North Atlantic, that the molecular phylogenetic study of Osborn et al. (2012) gave the following designations: genus A species 1, *Tergivelum* species 1, and genus D species 2. Our purpose here is to describe the morphology and biology of these three North Atlantic torquaratorids and to formally describe them. One of these worms is especially interesting because it is the first hermaphroditic species ever demonstrated in the phylum Hemichordata.

Methods

In the summer of 2003, manned *Mir I* and *Mir II* submersibles with their support ship, the R/V *Akademik Mstislav Keldysh*, explored the northern transform fault valley in the northwest sector of the Charlie-Gibbs Fracture Zone, which traverses the Mid-Atlantic ridge and runs approximately east-west at ~52°N (Fig. 1, dashed line). Still photographs made at that time showed enteropneusts fully exposed on the deep-sea floor. In the following year, the remotely operated vehicles (ROVs) *Aglantha* and *Bathysaurus* supported by the R/V *G.O. Sars* investigated wider areas of the Northern Mid-Atlantic Ridge (Wenneck et al. 2008) and obtained still photographs as well as video recordings of epibenthic enteropneusts. In June 2009, the ROV *Isis* supported by the RRS *James Cook* (cruise 36) made video recordings of several more deep-living enteropneusts. However, it was not until June 2010 that enteropneusts were both imaged

in the deep North Atlantic and then captured and brought to the surface for further study (Jones et al. 2010; Priede et al. 2012). This was accomplished by the ROV *Isis* supported by the RRS *James Cook* (ECOMAR cruise 48) at sites identified as NW, northwest; NE, northeast; SW, southwest; and SE, southeast (Fig. 1). At each site, enteropneusts were recorded in still or video images and then collected with a suction sampler (or less often, with a box core).

The freshly collected worms were quickly transferred to a ship-board aquarium in a temperature-controlled room at 6°C for color photography. Illumination was provided by a bilateral pair of daylight strobes placed equidistant from the specimens to ensure faithful recording of body color (Fig. 2C,E,H); this avoided the chromatic distortion that tends to result from the lighting conditions used for deep-sea photography and video recording. For nine collected enteropneusts of three species, Table 1 summarizes information on the collection and repository of the morphological holotypes and paratypes. In addition, this article includes information about the behavior of one enteropneust imaged but not collected during a video transect by the ROV *Isis*.

As soon as practicable after collection, each enteropneust was divided into a major and a minor portion. The former was fixed in 10% formalin-seawater for anatomical and histological study. For serial sectioning, body regions selected from the major portion were embedded in paraplast and cut 15 μm thick. Gonads, which tended to shatter when sectioned in paraplast, were embedded in Spurr's resin and sectioned 5 μm thick with a glass knife.
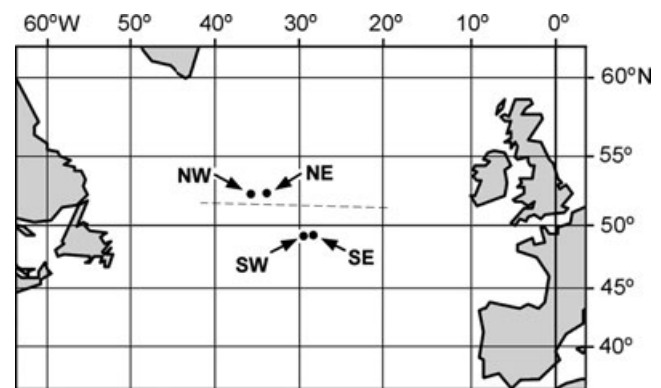
Fig. 1. Map of the North Atlantic, with the course of the Charlie-Gibbs Fracture Zone indicated by the dashed lines and the collection sites for the enteropneusts indicated by NW, NE, SW, and SE.
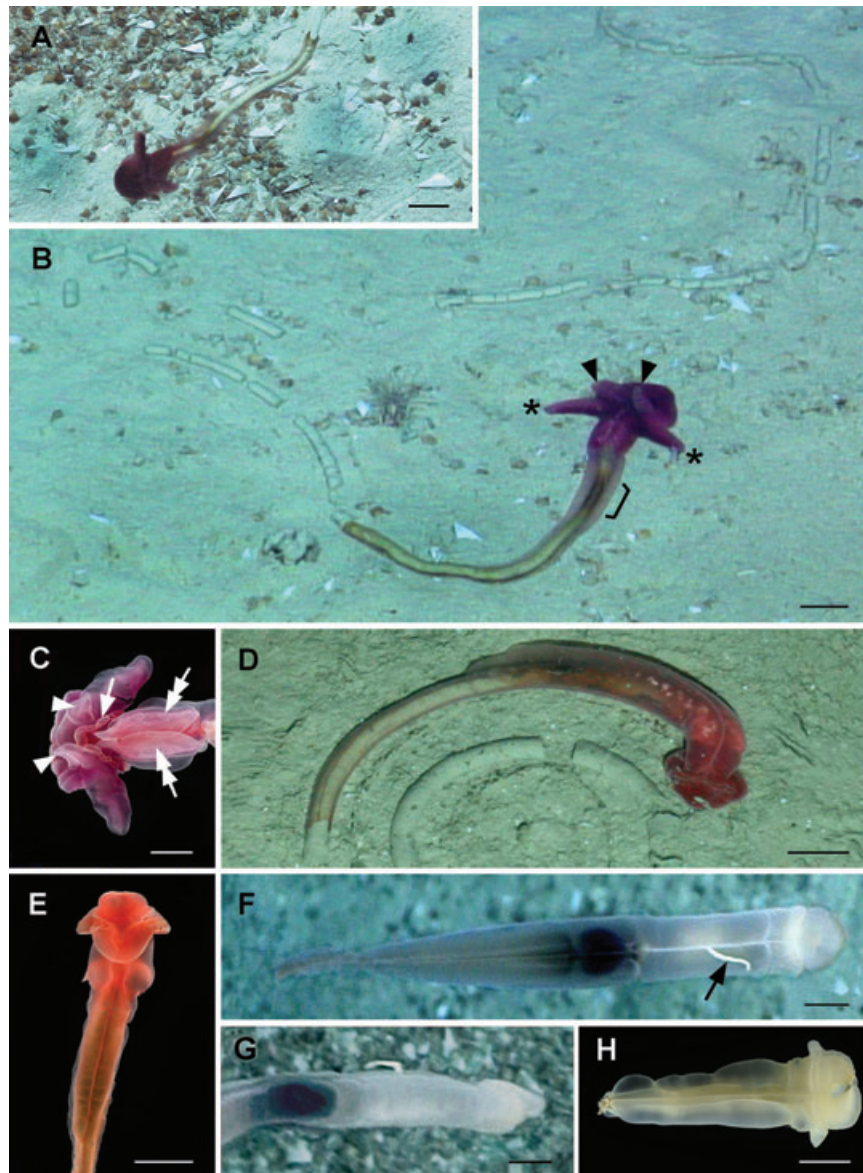
Fig. 2. Type specimens of *Yoda purpurata*, *Tergivelum cinnabarinum,* and *Allapasus isidis*. **A.** Holotype of *Y. purpurata* on the sea floor, in dorsal view. Scale bar=2 cm. **B.** Paratype 1 of *Y. purpurata* on the sea floor, in dorsal view; lateral lips and nuchal protuberances indicated, respectively, by arrowheads and asterisks, and the bracket shows the extent of the hepatic intestine. Scale bar=2 cm. **C.** Dorsal view of anterior end of paratype 3 of *Y. purpurata* fresh in chilled seawater after capture. Nuchal protuberances, posterior dorsal ridge, and genital wings are indicated, respectively, by arrowheads, single arrow, and tandem arrows. Scale bar=1 cm. **D.** Paratype 1 of *T. cinnabarinum* on bottom, in dorsal view. Scale bar=2 cm. **E.** Ventral view of anterior half of holotype of *T. cinnabarinum* fresh in chilled seawater after capture. Scale bar=2 cm. **F.** Holotype of *A. isidis* ~1 m above bottom, in dorsal view; a commensal/parasite (probably a leech) which was lost during collection is indicated by arrow. Scale bar=1 cm. **G.** Holotype of *A. isidis* photographed ~0.5 m above the bottom, in right-side view. Scale bar=1 cm. **H.** Dorsal view of anterior fourth of holotype of *A. isidis* fresh in chilled seawater after capture. Scale bar=1 cm.

Both the paraplast and Spurr sections were stained in 0.1% aqueous azure A.

The minor portion of each worm was transferred into 90% ethanol for later molecular analysis. DNA was extracted from ethanol-fixed material, amplified, sequenced, and analyzed as described by Osborn et al. (2012). The binomials of three North Atlantic enteropneusts described here are placed in the context of the phylogenetic analysis of Osborn et al. (2012), which was based on unlinked but

Table 1. Collection and repository data for holotypes and paratypes of *Yoda purpurata* n. gen., n. sp., *Tergivelum cinnabarinum* n. sp., and *Allapasus isidis* n. sp.

Genus and species (sex)	Date	Area/station/dive[a]	Longitude/latitude	Depth (m)	Color figures	Living length (cm)	Repository[b]
Yoda purpurata							
Holotype (hermaphrodite)	22 June 2010	SW/43/174	48.73°N/28.65°W	2622	2A	12	NHMUK 2011.7
Paratype 1 (not sectioned)	28 June 2010	SE/54/179	49.98°N/27.83°W	2759	2B	19	NHMUK 2011.8
Paratype 2 (not sectioned)	19 June 2010	SW/36/171	48.73°N/28.67°W	2502		13	NHMUK 2011.6
Paratype 3 (hermaphrodite)	19 June 2010	SW/36/171	48.73°N/28.67°W	2503	2C	15	NHMUK 2011.5
Tergivelum cinnabarinum							
Holotype (male)	7 June 2010	NW/17/163	53.99°N/36.19°W	2493	2E	12	NHMUK 2011.2
Paratype 1 (female)	8 June 2010	NE/24/165	54.02°N/34.15°W	2490	2D	20	NHMUK 2011.3
Paratype 2 (male)	12 June 2010	NE/28/168	54.02°N/34.18°W	2427		26	NHMUK 2011.4
Paratype 3 (not sectioned)	6 June 2010	NW/16/162	53.99°N/36.19°W	2493	(1i)[c]	11	NHMUK 2011.1
Allapasus isidis							
Holotype (male)	22 June 2010	SW/43/174	48.73°N/28.65°W	2622	2F–H	13	NHMUK 2011.9

[a]Area in Fig. 1; RRS *James Cook* stations (Cruise 48) and ROV *Isis* dive numbers from Jones et al. (2010).
[b]Natural History Museum London, UK, Lower Invertebrates Curation Group.
[c]Figure 1i is in Osborn et al. (2012).

concatenated complete 18S and partial 16S nucleotide sequences of hemichordates and outgroup echinoderms. The consensus tree was established by a 90% majority rule from Bayesian analysis (50 million generations).

Results

Systematic accounts

Phylum Hemichordata BATESON 1885
Class Enteropneusta GEGENBAUR 1870

Fig. 3. *Yoda purpurata* n. gen., n. sp. All photos show holotype. **A.** Drawing of worm in dorsal view; anterior toward right. **B.** Fixed worm. The fragment at the top shows a dorsal view of the anterior end (toward the left), twisting to a ventral view of the trunk; the bottom fragment shows a ventral view of the anterior (toward the right) twisting to a dorsal view of the trunk. The arrowhead indicates the mouth closed to a narrow slit; the arrow indicates the posterior lip. The levels of the cross sections in C–J are indicated. Scale bar=1 cm. **C.** Cross section at level of genital wings (arrowhead) and pharynx, which is divided into a dorsal, respiratory region (twin asterisks), and a ventral digestive region (single asterisk); ovaries and testes are associated with the concave surface of the genital wing. Scale bar=1 mm. **D.** Testes (arrow) and ovaries (arrowheads) associated with the epithelium covering the genital wing. Scale bar=200 μm. **E.** Cross section through prehepatic intestine; the dorsal and ventral nerve cords are indicated by the arrowhead and arrow, respectively, and the ventral folds are indicated by asterisks. Scale bar=1 mm. **F.** Unstained enlargement of E. Intestinal epithelial cells (top) lack intrinsic pigmentation. Scale bar=100 μm. **G.** Cross section through hepatic intestine. Dorsal and ventral nerve cords are indicated by the arrowhead and arrow, respectively, and the ventral folds are indicated by asterisks. Scale bar=2 mm. **H.** Unstained enlargement of G showing intestinal epithelial cells (top) crowded with dark brown granules. Scale bar=100 μm. **I.** Gut contents in hepatic intestine. Scale bar=50 μm. **J.** Cross section through posthepatic intestine. Dorsal and ventral nerve cords are indicated by the arrowhead and arrow, respectively, and ventral folds are indicated by asterisks. Scale bar=1 mm. Adr, anterior dorsal ridge; an, anus; co, collar; dnc, dorsal nerve cord; gw, genital wing (overlying pharyngeal region of trunk); hi, hepatic intestine; lli, lateral lip; lvf, lateroventral fold; np, nuchal protuberance; pdr, posterior dorsal ridge; pohi, posthepatic intestine; pr, proboscis; prhi, prehepatic intestine.
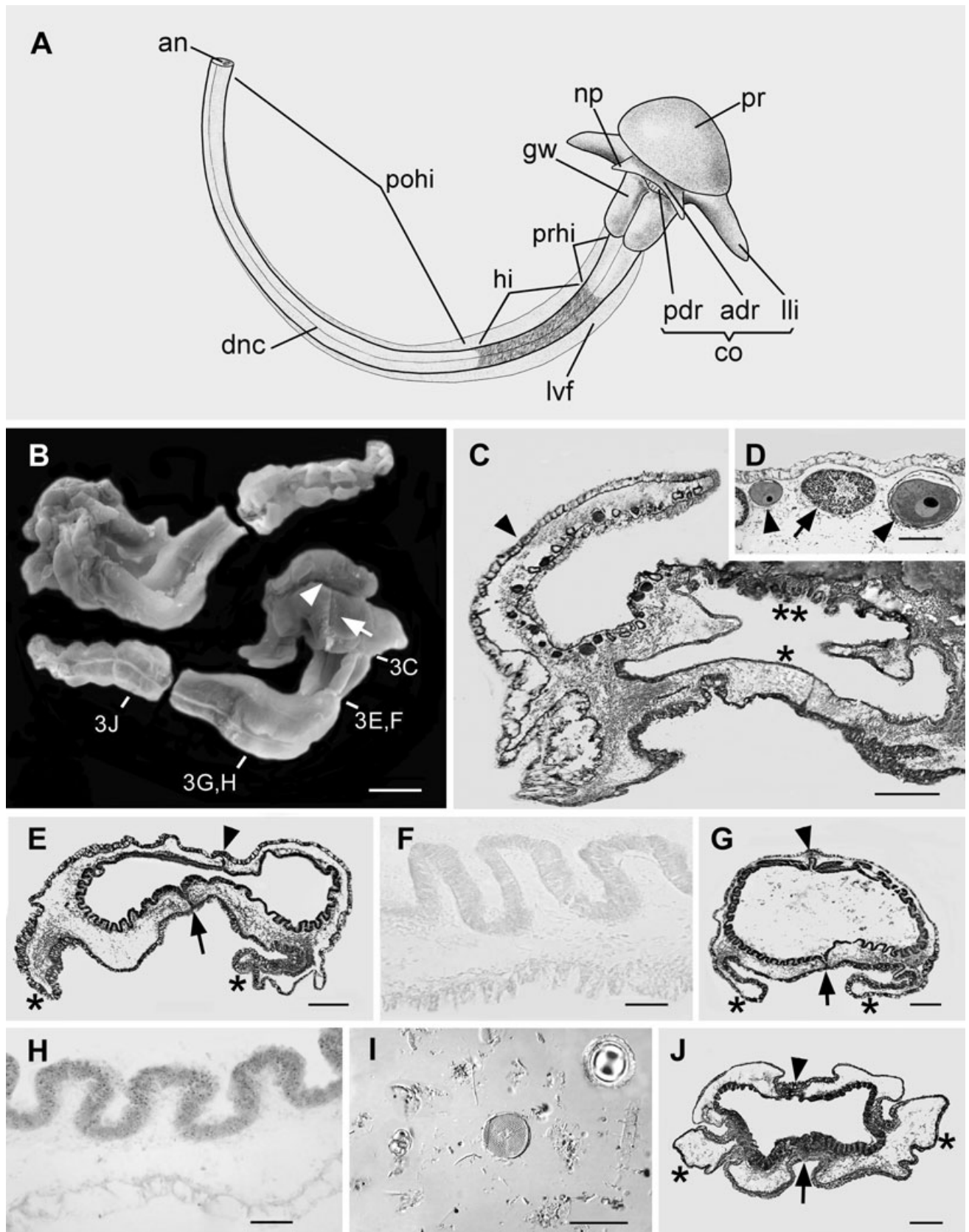
Family Torquaratoridae HOLLAND ET AL. 2005
(re-diagnosed by Osborn et al. 2012)
Yoda n. gen.

Diagnosis of genus. Two thirds of the width of the collar is accounted for by a pair of gradually tapering lateral lips, each three times longer than its anterior/posterior dimension basally. A conical nuchal protuberance projects dorsally from the anterior dorsal ridge of the collar on either side of the midline.

Type species. *Yoda purpurata* n. sp.

Etymology of generic name. *Yoda* refers to the lateral lips, which are shaped like the ears of Yoda, a character in the Star Wars universe.

Yoda purpurata n. gen., n. sp. (Figs. 2A–C, 3)

Synonymy. "North-Atlantic form" in Holland et al. (2005). "Rosy acorn worm" in nationalgeographic.com/news/2011/11/pictures/111121. "Genus A, species 1" in Osborn et al. (2012).

Type material. Holotype: RRS *James Cook* Cruise 048 Station 43, ROV *Isis* dive 174, 2622 m, 48.73°N, 28.65°W, 22 June 2010, I. G. Priede, formalin-fixed hermaphrodite prepared as serial cross sections. Repository: NHMUK 2011.7. Collection and repository data for paratypes 1–3 are in Table 1. At the time of collection, the holotype and paratypes were browsing completely exposed on the sea floor.

Diagnosis of species. Photographed freshly collected under daylight strobe illumination (Fig. 2C), the proboscis, collar, and genital wings of trunk (pr, co, gw, respectively, in Fig. 3A) are dark reddish purple (fuschia); more posterior trunk tissues are only slightly tinged with purple.

Etymology of specific name. *purpurata* is a Latin adjective meaning purple.

Description, external. The living holotype, as determined from deep-sea video images, was 12 cm long (paratypes 1–3, respectively, were 19, 13, and 15 cm long). As mentioned in the diagnosis, the anterior body regions of the living worm are reddish purple; by contrast, more posteriorly in the trunk, the tissues are only slightly tinged with purple, and the beige gut contents are visible through the thin body wall (Fig. 2A,B), except where the color of the brownish endoderm of the hepatic intestine (Fig. 2B, bracket) predominates.

In situ images of the living worm show the proboscis has the shape of a smooth dome ~2 cm long by 3.5 cm wide. Following capture (Fig. 2C) and fixation (Fig. 3B), the proboscis appears shrunken and wrinkled. As seen in dorsal view, the collar of the living worm is ~0.5 cm long by 6 cm wide, and

is made up of the structures diagramed in Fig. 3A (co). Two thirds of the collar width is accounted for by the bilaterally paired, tapering lateral lips (Fig. 2B, asterisks; Fig. 3A, lli). The collar also comprises a posterior dorsal ridge with a very narrow anterior/posterior dimension (Fig. 2C, arrow) and a somewhat wider anterior dorsal ridge that bears a pair of nuchal protuberances (Fig. 2B,C, arrowheads; Fig. 3A, np). On the ventral side of the collar, the mouth of the holotype (Fig. 3B, arrowhead) is closed and somewhat distorted. The ventromedial portion of the collar is the mouth's posterior lip (Fig. 3B, arrow).

The chief components of the trunk are diagramed in Fig. 3A. When the trunk is regarded in dorsal view, the genital wings (Fig. 2C, tandem arrows; Fig. 3A, gw) have an anterior/posterior length of ~2 cm. Genital wings are sheet-like folds of the body wall arising laterally from either side of the pharyngeal region and arching over it dorsally such that their edges meet in the dorsal midline. Posterior to the pharyngeal region, the trunk measures ~14.5 cm long by 0.7 cm wide (discounting the lateroventral folds) and is regionalized into relatively short prehepatic and hepatic intestinal regions, followed by a relatively long posthepatic intestine. Along either side of the postpharyngeal trunk, a lateroventral fold ~0.7 cm wide runs along the prehepatic and hepatic intestinal regions; it gradually narrows along the posthepatic intestinal region to a width of only 0.1 cm near the posterior extremity of the trunk, where the anus opens.

Description, internal. The epidermis covering the proboscis (in common with that of the rest of the body) consists of slender support cells and abundant mucous gland cells. The intraepidermal nervous system of the proboscis is ubiquitous, but most conspicuous mid-dorsally along the proboscis stalk. The proboscis coelom is occupied by a diffuse mesh of smooth muscle and connective tissue cells (the pigment granules in these cells retain a red color even after successive exposure to ethanol and xylene). No coelomopores were detected connecting the proboscis coelom with the exterior, but their absence needs to be verified by studying additional specimens. As in other torquaratorid enteropneusts, excepting those in the genus *Allapasus* (Holland et al. 2012; present study), there is no evidence of the skeleton–heart–kidney–stomochord complex in the proboscis stalk.

In the collar region of the holotype of *Y. purpurata,* some internal features of the dorsomedial region were disrupted by extensive swelling of epidermal mucous cells during fixation; the copious mucus was

also unusually tough, making histological sectioning difficult. Thus, the collar nerve cord and its associated structures cannot be described here. The lips, anterior dorsal ridge with nuchal protuberances, and posterior dorsal ridge of the collar resemble the proboscis in consisting of a mucus cell-rich epithelium enclosing a diffuse meshwork of muscles and connective tissue cells. No coelomopores were found in the collar region, but their absence needs to be established definitively if specimens with better preservation in the dorsal collar region come to hand.

The subdivisions of the trunk, from anterior to posterior, are the gonadal wings (coextensive with the underlying pharynx), prehepatic intestine, hepatic intestine, and posthepatic intestine (Fig. 3A, gw, prhi, hi, and pohi, respectively). The genital wings, which comprise a covering of epidermis over a sparse meshwork of connective tissue and smooth muscle cells, arch over the body, thus hiding the dorsal surface of the pharyngeal region where the gill pores penetrate. The gonads are closely associated with the concave surface of each genital wing (Fig. 3C). Separate ovaries and testes, in roughly even numbers, were found together in both the holotype and paratype 3 of *Y. purpurata*, the first hermaphrodites ever demonstrated in the phylum Hemichordata. Each ovoid testis (Fig. 3D, arrow) is ~300 μm in average diameter and comprises a peripheral zone of spermatogenic cells surrounding a lumen containing sperm cells. The head of each sperm is approximately spherical with a diameter of 2–3 μm. The ovaries (Fig. 3D, arrowheads) each consist of a thin germinal epithelium surrounding a single primary oocyte with a conspicuous nucleus (germinal vesicle) containing a prominent nucleolus. The oocytes are of various sizes, the largest having a diameter of ~300 μm.

Cross sections of the pharynx show a dorsal branchial zone (Fig. 3C, twin asterisks) incompletely separated from a ventral digestive zone (Fig. 3C, single asterisk) with a relatively smooth lining. The arrangement of the primary and secondary gill bars in the dorsal roof of the branchial zone was disrupted by the swelling of nearby epidermal mucous cells; however, there were no indications that the gill bars were interconnected by synapticles. Because of this disruption, it was not possible to count the gill pores accurately, but they numbered at least several dozen. In the trunk posterior to the genital wing/ pharyngeal subdivision, the digestive tract included no histologically distinct esophagus separating the pharynx from the more posterior intestine.

The prehepatic, hepatic, and posthepatic intestines have much in common structurally. They are accompanied by the dorsal nerve cord, ventral nerve cord, and lateroventral folds (arrowheads, arrows, and asterisks, respectively, in Fig. 3E,G,J) and their lining endoderm is corrugated by ~15 plicae on either side of the midline (each plica runs ventroanteriorly at a 45° angle from the dorsal to the ventral midline). In unstained sections, the endodermal cells lining the prehepatic and posthepatic intestine are almost invisible (Fig. 3F), whereas the cells lining the hepatic intestine are relatively conspicuous (Fig. 3H) due to their content of numerous dark brown granules ~1 μm in diameter. The hepatic intestine of *Y. purpurata*, in contrast to that of some other enteropneusts, lacks sacculations. Most of the gut contents of the holotype evidently spilled out when the worm broke apart during collection. However, the lumen of the hepatic intestine contained some flocculent material plus a scattering of skeletal remains of sponges, diatoms, and foraminifera, in addition to some unidentified cysts (Fig. 3I).

Behavior. The browsing path of *Y. purpurata*, as traced by its fecal trail, meanders irregularly over the deep-sea floor (Fig. 2B). In video recordings showing collection of the worms, the ventral side of the body appeared strongly adherent to the substratum, possibly due the secretion of exceptionally sticky mucus.

Genus *Tergivelum* HOLLAND ET AL. 2009
Type species *Tergivelum baldwinae*
HOLLAND ET AL. 2009

***Tergivelum cinnabarinum* n. sp.** (Figs. 2D,E, 4)

Synonymy. "Second North-Atlantic form" in Holland et al. (2005). "*Tergivelum* species 1" in Osborn et al. (2012).

Type material. Holotype: RRS *James Cook* Cruise 048 Station 17, ROV *Isis* dive 163, 2493 m, 53.98° N, 36.20°W, 7 June 2010, I. G. Priede, formalin-fixed male prepared as serial cross sections. Repository: NHMUK 2011.2. Collection and repository data for paratypes 1–3 are in Table 1. At time of collection, the holotype and paratypes were browsing completely exposed on the sea floor; all specimens were imaged at depth with back veils, but these were evidently lost during collection.

Diagnosis of species. Photographed freshly collected under daylight strobe illumination (Fig. 2E), proboscis and collar are the color of cinnabar (=vermilion); more posterior trunk regions pale orange. This body color contrasts with that of morphologically similar congener, *Tergivelum baldwinae*, in which the anterior body regions are dark brown.
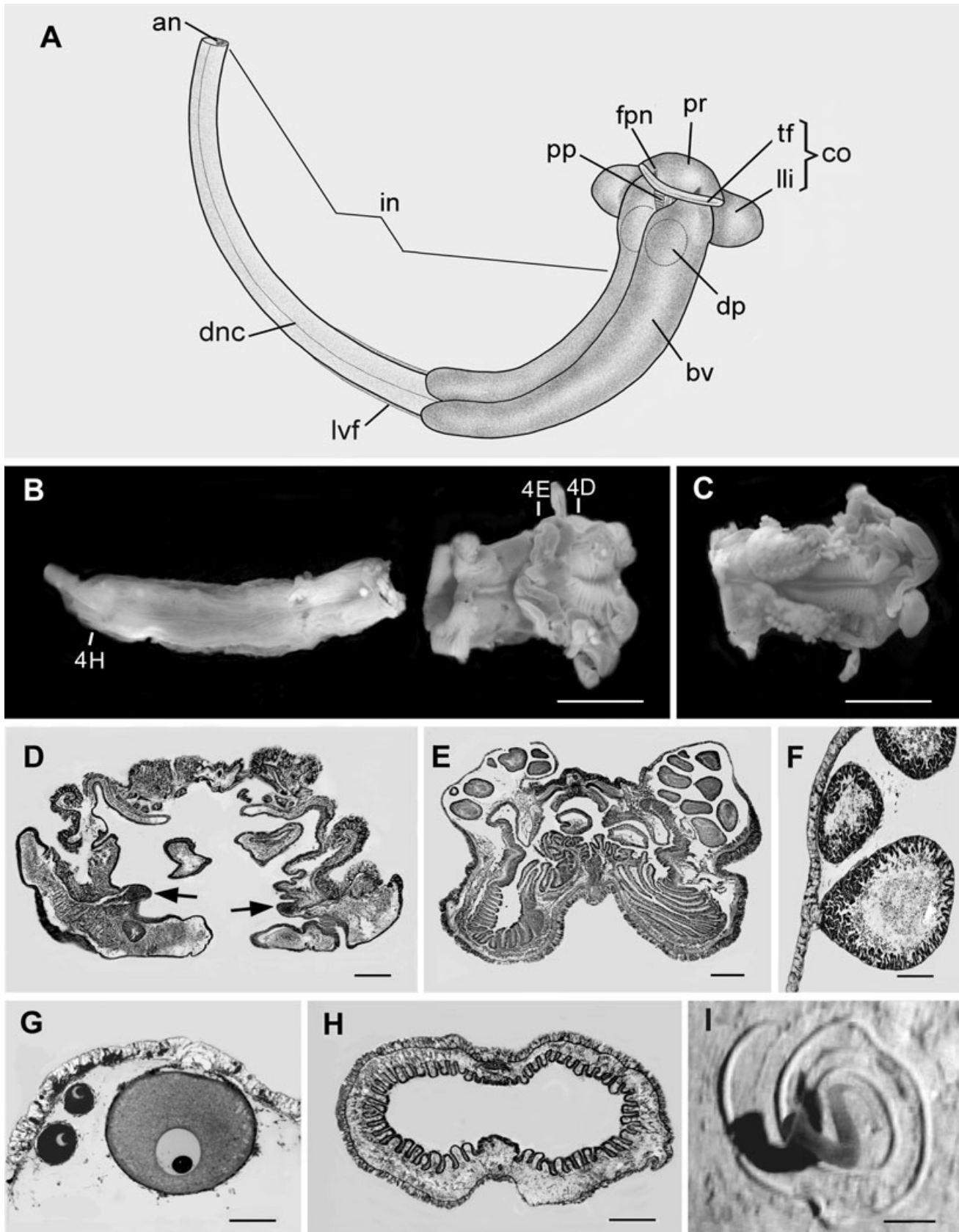
Etymology of specific name. *Cinnabarinum* is the Latin adjective for cinnabar (vermilion).

Description, external. The length of the living holotype, as determined from deep-sea video images, was 12 cm (and paratypes 1–3 were, respectively, 20, 26, and 11 cm long). As mentioned in the diagnosis, the anterior body regions are the color of cinnabar, while the more posterior body is a light orange (with beige gut contents showing through). The relative proportions of the body regions (Figs. 2D, 4A–C), including the back veils, which are diagnostic of the genus, are similar to those of *T. baldwinae* (Holland et al. 2009).

Description, internal. The internal anatomy of *T. cinnabarinum* is very similar to that already described for *T. baldwinae* by Holland et al. (2009), and only features of special significance will be described here. The conspicuous right and left buccal muscles (Fig. 4D, arrows) on either side of the mouth are diagnostic of the genus *Tergivelum*. The holotype is a male with numerous testes located in the dorsal protuberances (top right and top left in Fig. 4E). Each testes is ovoid (Fig. 4E,F) and has an average diameter of ~300 μm. The germinal epithelium of the testis comprises immature germ cells, while the sperm cells in the lumen have approximately spherical heads with a diameter of 2–3 μm. The two paratypes are females with numerous ovaries associated with the epidermis covering the dorsal protuberances (Fig. 4G). Most of the ovaries contain a single primary oocyte characterized by a large nucleus (germinal vesicle) containing a prominent nucleolus. The oocytes are of various sizes, none larger than ~400 μm in diameter. There were no gut contents in the lumen of any gut region (e.g., Fig. 4H), presumably due to loss during collection and histological processing.

Behavior. The browsing pattern of *T. cinnabarinum*, as indicated by its fecal trail, begins as a spiral (as judged from *in situ* photographs of seven different individuals) that is sometimes continued as a switchback pattern. During one video transect, an evidently undisturbed specimen of *T. cinnabarinum* (Fig. 4I) was imaged during *Isis* dive 168. The worm, visible for ~7 s as the ROV passed 2 m above it at 13 cm s^{-1}, was positioned with its proboscis, collar and most of the trunk almost vertical in the water column, and was evidently just ascending above its browsing site on the sea floor.

Genus *Allapasus* Holland et al. 2012
Type species *Allapasus aurantiacus*
Holland et al. 2012
***Allapasus isidis* n. sp.** (Figs. 2F–H, 5)

**Synonymy.** "Genus D, species 2" in Osborn et al. (2012).

Type material. Holotype: RRS *James Cook* Cruise 048 Station 43, ROV *Isis* dive 174, 2622 m, 48.73°N, 28.65°W, 22 June 2010, I. G. Priede, formalin-fixed hermaphrodite prepared as serial cross sections. Repository: NHMUK 2011.9. When first observed, the holotype was floating in the water column ~1 m above the bottom. There are no paratypes.

Diagnosis of species. Photographed freshly collected under daylight strobe illumination, the body color is light yellow (Fig. 2H), which contrasts with the light orange color of its congener, *A. aurantiacus*.

Etymology of specific name. *Isidis* is a genitive form of the Latin noun *Isis* (Salem 1938), the name of the ROV that collected the holotype.
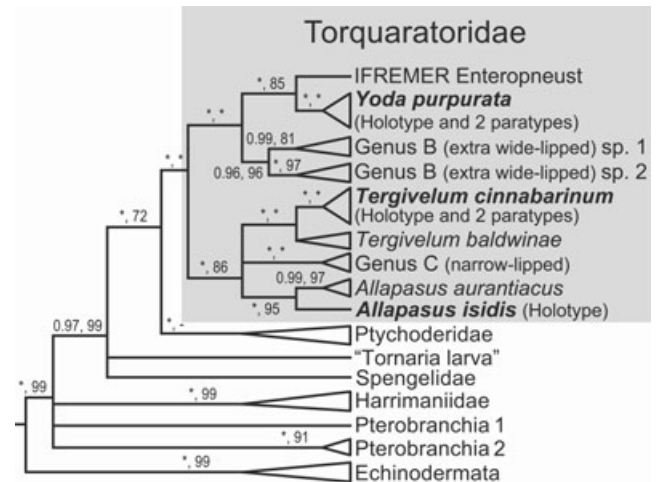
Description, external. The length of the living holotype, as determined from deep-sea video imagery, was 13 cm. As mentioned in the diagnosis, the living color of the body is light yellow (the white body color in Fig. 2F,G is an artifact created by the light sources used during the deep-sea imaging). In the region of the hepatic intestine (Fig. 5A, hi), the dark brown gut wall shows through the body wall (Figs. 2F,G, 5B). The overall body shape is more compact in *A. isidis* than in *A. aurantiacus*, the length-to-width ratio of the former being only about half that of the latter. The edges of the lateral wings were in contact with each other mid-dorsally all along the trunk in the undisturbed holotype (Fig. 2F), but spread apart (Fig. 4B, arrow) on the close approach of the ROV.

Fig. 4. *Tergivelum cinnabarinum* n. sp. B–F and H show holotype. **A.** Drawing of worm in dorsal view; anterior toward right. **B.** Fixed holotype in ventral view, with anterior toward the right. The levels of the cross sections in D–H are indicated. Scale bar=1 cm. **C.** Fixed holotype. Dorsal view of anterior end, with back veils torn away. Scale bar=1 cm. **D.** Cross section through the buccal cavity showing the conspicuous buccal muscles (arrows). Scale bar=1 mm. **E.** Cross section through the dorsal protuberances (top right and top left) containing the gonads. Scale bar=1 mm. **F.** Testes of holotype. Scale bar=200 μm. **G.** Ovaries of paratype 1. Scale bar=100 μm. **H.** Cross section near the posterior end of intestine. Scale bar=1 mm. **I.** Living specimen of *T. cinnabarinum* (not collected) observed at 2480 m ascending into the water column. Scale bar=3 cm. An, anus; bv, back veil; co, collar; dp, dorsal protuberance; fpn, fossa of proboscis nerve; in, intestine; lli, lateral lip; pp, pharyngeal pores; pr, proboscis; tf, transverse fold.
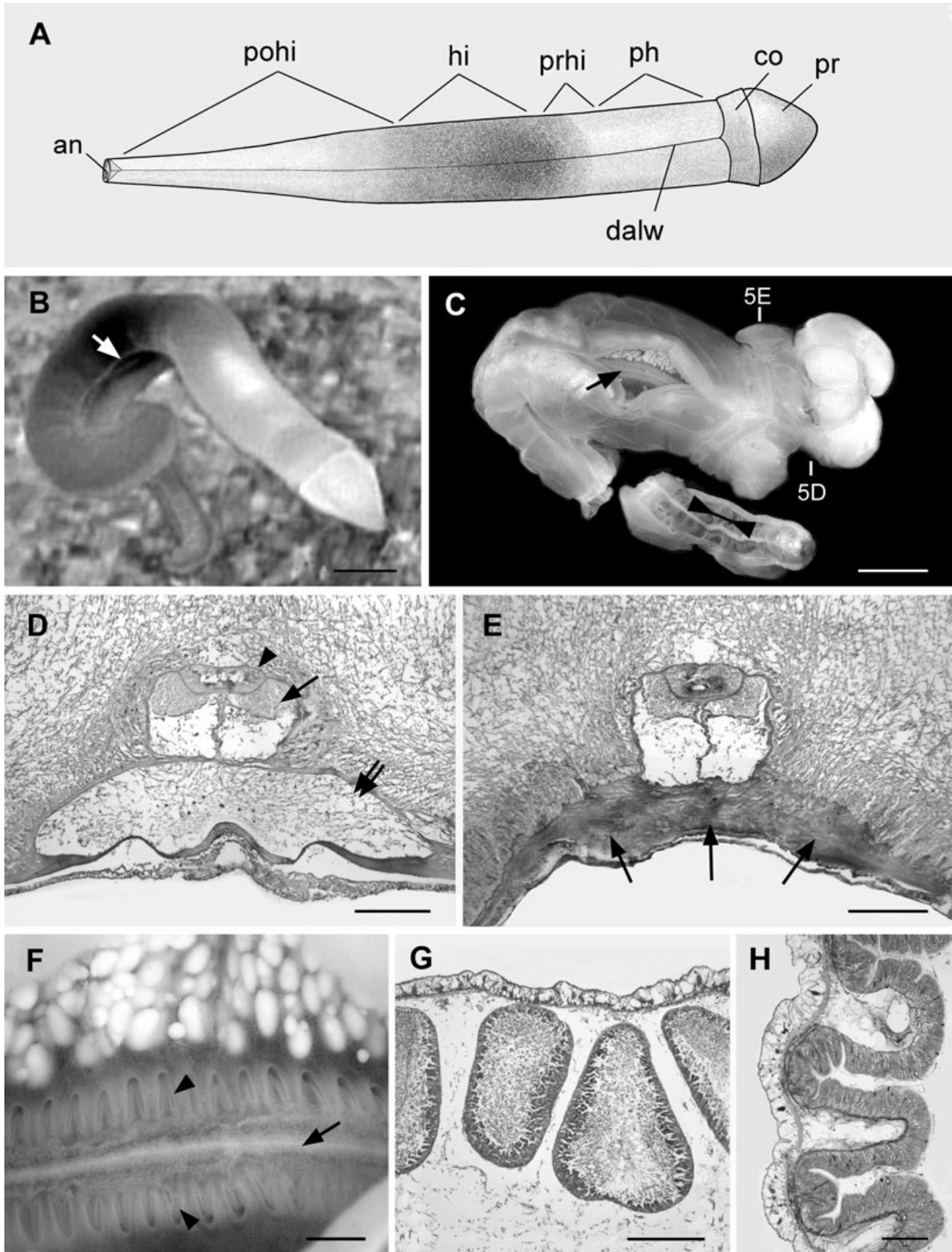
Description, internal. The internal anatomy of *A. isidis* is very similar to that already described for *A. aurantiacus* by Holland et al. (2012), and only features of special interest will be described here. The stomochord (Fig. 5D, twin arrow), which is packed with a mass of vacuolated cells and lacks a detectable lumen, is virtually identical to its appearance in *A. aurantiacus* (Holland et al. 2012). More posteriorly in the collar, a small, plate-like proboscis skeleton (Fig. 5E, arrows) separates the stomochord from the main course of the digestive tract, again just as in *A. aurantiacus* (Holland et al. 2012). The dorsal side of the pharyngeal region of the trunk is characterized by a row of gill pores running on either side of the dorsal nerve cord (Fig. 5C,F, arrow). Lateral to the gill pores, hundreds of testes, with diameters up to ~500 μm, are visible through the overlying epidermis. Each testis (Fig. 5G) comprises a peripheral zone of immature spermatogenic cells and a central lumen filled with mature sperm. The approximately spherical head of each sperm has a diameter of 2–3 μm. The only known specimen of *A. isidis* is the male holotype; presumably this species is gonochoric, and female specimens will ultimately be discovered. No histologically specialized esophagus intervenes between the pharynx and intestine. The prehepatic intestine, hepatic intestine (which is sacculate, Fig. 5H), and posthepatic intestine resemble the corresponding intestinal regions in *A. aurantiacus*. No gut contents were found in the lumen of any part of the digestive tract of the holotype of *A. isidis*.

Behavior. Because the holotype was not crawling on the bottom when observed at depth, nothing is known about its fecal trail (if it even produces one). Because observations were limited to the holotype, it is also not known if *A. isidis* can burrow shal-

lowly as has been demonstrated for its congener, *A. aurantiacus* (Holland et al. 2012).

Phylogenetics

The three new species described here are placed within the context of an overall tree of hemichordates in Fig. 6. The three new taxa cluster with previously described species in the family Torquaratoridae. This family, which so far comprises deep-sea species exclusively, is the sister to the Ptychoderidae.

Fig. 6. Phylogenetic tree showing the relationships of the three species described here to other Torquaratoridae (shaded area of tree) and other enteropneusts previously studied by Osborn et al. (2012). At each branch, the first support value indicates posterior probabilities from the Bayesian analysis and the second bootstrap support from parsimony analysis. Asterisks indicate support values of 1.0 or 100%, respectively.

Fig. 5. *Allapasus isidis* n. sp. **A.** Drawing of worm in dorsal view; anterior toward right. **B.** Living worm just above bottom, with the body somewhat twisted by the approach of the ROV. The arrow indicates where the lateral wings on either side of the dorsal midline have pulled apart to reveal the region of the hepatic intestine. Scale bar=1 cm. **C.** Fixed worm in dorsal view, with anterior at top right; the levels of the cross sections in D and E are indicated. An enlargement of the region where the lateral wings are pulled apart (arrow) is in F. A broken fragment comprising the hepatic intestine is at bottom center; the line between the arrowheads is the orientation of the section in H. Scale bar=1 cm. **D.** Cross section through the collar showing the dorsal nerve cord (arrowhead), perihaemal coelom with muscles (single arrow), and stomochord (twin arrow). Scale bar=200 μm. **E.** Cross section through the collar at the level where the proboscis skeleton (arrows) separates the stomochord (beneath the plane of this section) from the rest of the digestive tract. The skeleton shown here is a composite of the skeleton in three successive cross sections. Scale bar=200 μm. **F.** Enlargement of the arrowed region in C; the testes are visible at top through translucent ectoderm, and the gill pores (arrowheads) run on either side of dorsal nerve cord (arrow). Scale bar=1 mm. **G.** Cross section of testes beneath the ectoderm (at top). Scale bar=200 μm. **H.** Hepatic intestine in parasagittal section (corresponding to the line between the arrowheads in C); intestinal lumen at right, ectoderm at left. Scale bar=200 μm. An, anus; co, collar; dalw, dorsal apposition of the lateral wings; hi, hepatic intestine region; ph, pharyngeal region; pohi, posthepatic intestine region; pr, proboscis; prhi, prehepatic intestine region.

Discussion

The three new species described here bring to six the number of described species in the family Torquaratoridae, although that number can be expected to increase substantially in the near future. First, several species already characterized by their rDNA sequences (i.e., the unnamed species in Fig. 6) are being described morphologically; second, additional specimens have been collected (our unpubl. data from the Russian Arctic and Gulf of California) and are awaiting both molecular and morphological analysis; and third, no torquaratorid has yet been collected from anywhere in the South Atlantic, South Pacific, or Indian Oceans, although many have been imaged at depth in those regions (e.g., table 1 in Smith et al. 2005; Anderson et al. 2011). Thus, it is possible that the family Torquaratoridae, in spite of its relative inaccessibility, will eventually outstrip all the other enteropneust families in number of described species.

The present description of three additional torquaratorid species has provided insights into what influences their foraging patterns. Presumably, these patterns are influenced in part by local environmental conditions and in part by taxon-specific behaviors. Smith et al. (2005) and Anderson et al. (2011) stressed environmental influences. For example, it is reasonable to propose that worms on a nutrient-rich patch of sediment would browse in a pattern (e.g., a spiral) tending keep them there as long as possible. Even so, the results of this study indicate that taxon specificity may be more influential than previously suspected. For example, specimens of *Yoda purpurata* in the North Atlantic (present study) and its likely congeners (yet to be described) in the Pacific (Thiel 1979; Anderson et al. 2011) browse in an irregular, meandering path. In contrast, specimens of *T. cinnabarinum* in the North Atlantic (present study), *T. baldwinae* in the East Pacific (Holland et al. 2009), and their undescribed congeners in the West Pacific and Indian Oceans (table 1 in Smith et al. 2005; Anderson et al. 2011) begin browsing along a spiral path that not infrequently transitions into a switchback pattern. It is likely that a worm in the genus *Tergivelum* is enabled to steer a precise course by its highly developed bilateral proboscis nerves and buccal muscles, whereas a worm in the genus *Yoda*, with its more rudimentary neuromuscular development, simply cannot sense its environment acutely enough nor control its movements precisely enough to travel in a spiral or tight switchback pattern. It will be interesting to see how descriptions of additional torquaratorids will clarify the relationship between morphological structure and detailed foraging behavior.

Although more torquaratorid species are being described, little is yet known about their natural history. For instance, browsing epibenthically would seem to expose the worms to predation, but there is at present no definite information on whether they might be protected chemically or physically (e.g., by a thick coat of clear mucus). Another key question is how the worms alternate between epibenthic crawling and floating in the water column. The ascent from the bottom (Fig. 4I) involves jettisoning of gut content ballast (Smith et al. 2005), elevating the anterior portion of the body, and perhaps production of a mucus coating or parachute (Holland et al. 2009; Osborn et al. 2012). Nothing definite is known about the mechanics of the descent back down to the sea floor. The process could well be passive in the sense that a floating worm may simply settle to the bottom when the ambient current slows down. On the other hand, more active possibilities could include expulsion of buoyant body or gut fluid, shedding of an external mucus envelope, or muscle-driven postural changes. However, because the musculature of torquaratorids is only weakly developed, it is very unlikely that descent involves active swimming of the sort known for one shallow water enteropneust (Urata et al. 2012).

Within a given torquaratorid species, individual worms presumably interact, but such interactions have yet to be observed directly. Presumably such interactions would be between individuals on the sea floor, because the chances that they could ever get together while floating appear vanishingly small. Torquaratorids studied to date are characterized by low population densities, as might be predicted for browsers on energy-poor deep-sea deposits. For example, the highest density found during a 15-year study of *T. baldwinae* was two worms per 1000 m^2 (Smith et al. 2005), and the highest density ever recorded (for a mixture of Australian torquaratorid species) was 29 worms per 1000 m^2 (Anderson et al. 2011). The low density of torquaratorids presumably affects their reproductive biology. It is very unlikely that torquaratorids spawn at a long distance from one another while in their usual widely dispersed state. Instead, it is much more probable that sexually mature worms associate with one another, in pairs, as demonstrated for a deep-living echinoid by Young et al. (1992), or even more gregariously in reproductive hot spots (in the terminology of Drazen et al. 2003). In most torquaratorids studied so far, the sexes are separate, and it is likely that a male/female pair forms before the

gametes are emitted. Nothing in the structure of the worms described to date suggests that elaborate copulation takes place, although it is quite possible that the male and female shed their gametes within a common cocoon of mucus to facilitate fertilization.

In deep-sea benthic environments (aside from vents and seeps), animal populations are typically diffusely distributed. Under such conditions, hermaphroditism tends to be common to increase the probability of finding a suitable mate. Surprisingly, however, prior to the present study, this mode of reproduction was unknown in any member of the family Torquaratoridae—and, in fact, was unknown for the entire phylum Hemichordata. Here, we have shown that *Y. purpurata* is hermaphroditic, a feature that certainly must ameliorate the problem of rare encounters between individuals in the deep sea. With the description of additional torquaratorid species (especially in the genus *Yoda*), it will be interesting to determine the frequency of hermaphroditism within the family. Additional collections of torquaratorids may also help clarify the function of the peculiar externalized ovaries previously described for *A. aurantiacus* (Holland et al. 2012). Although this study includes the congeneric *A. isidis*, the only known specimen is a male and sheds no further light on this problem.

References

Anderson TJ, Przeslawski R, & Tran M 2011. Distribution, abundance and trail characteristics of acorn worms at Australian continental margins. Deep-Sea Res. II 58: 970–978.

Bateson W 1885. Note on the later stages in the development of *Balanoglossus kowalevskii* (Agassiz), and on the affinities of the Enteropneusta. Proc. R. Soc. Lond. B 38: 23–30.

Cannon JT, Rychel AL, Eccleston H, Halanych KM, & Swalla BJ 2009. Molecular phylogeny of hemichordates, with updated status of deep-sea enteropneusts. Mol. Phylogenet. Evol. 52: 17–24.

Drazen JC, Goffredi SK, Schlining B, & Stakes DS 2003. Aggregations of egg-brooding deep-sea fish and cephalopods on the Gorda Escarpment: a reproductive hot spot. Biol. Bull. 205: 1–7.

Gee H 1996. Before the Backbone. Chapman & Hall, London. 347 pp.

Gegenbaur C 1870. Grundzüge der vergleichenden Anatomie, Zweite Auflage. Engelmann, Leipzig. 892 pp., 319 Holzschnitte.

Hall BK 2005. Betrayed by *Balanoglossus*: William Bateson's rejection of evolutionary embryology as the basis for understanding evolution. J. Exp. Zool. B 304: 1–17.

Holland ND, Clague DA, Gordon DP, Gebruk A, Pawson DL, & Vecchione M 2005. "Lophenteropneust" hypothesis refuted by collection and photos of new deep-sea hemichordates. Nature 434: 374–376.

Holland ND, Jones WJ, Elena J, Ruhl H A, & Smith KL 2009. A new deep-sea species of epibenthic acorn worm (Hemichordata, Enteropneusta). Zoosystema 31: 333–346.

Holland ND, Kuhnz LA, & Osborn KJ 2012. Morphology of a new deep-sea acorn worm (Class Enteropneusta, Phylum Hemichordata): a part-time demersal drifter with externalized ovaries. J. Morphol. 273: 661–671.

Jones D, Alt C, Gebruk A, Rogacheva A, & Gooday A 2010. ROV video transects. In: RSS James Cook Cruise 048. ECOMAR Ecosystem of the Mid-Atlantic Ridge at the Sub-Polar Front and Charlie Gibbs Fracture Zone. Priede IG & Bagley PM, eds., pp. 65–80. Oceanlab, University of Aberdeen, Aberdeen, UK.

Lowe CJ 2008. Molecular genetic insights into deuterostome evolution from the direct-developing hemichordate *Saccoglossus kowalevskii*. Philos. Trans. R. Soc. Lond. B 363: 1569–1578.

Newell GE 1952. The homology of the stomochord of the Enteropneusta. J. Zool. 121: 741–746.

Osborn KJ, Kuhnz LA, Priede IG, Urata M, Gebruk AV, & Holland ND 2012. Diversification of acorn worms (Hemichordata, Enteropneusta) revealed in the deep sea. Proc. R. Soc. Lond. B 279: 1646–1654.

Priede IG, Billett DSM, Brierley AS, Hoelzel AR, Inall M, & Miller P 2012. The ECO-MAR (Ecosystem of the Mid-Atlantic Ridge at the Sub-polar Frond and Charlie Gibbs Fracture Zone) project and description of the benthic sampling programme 2007–2010. Mar. Biol. Res., in press.

Salem MS 1938. Ennius and the "Isiaci coniectores." J. Roman Stud. 28: 56–59.

Smith KL, Holland ND, & Ruhl HA 2005. Enteropneust production of spiral fecal trails on the deep-sea floor observed with time-lapse photography. Deep-Sea Res. I 52: 1228–1240.

Spengel JW 1893. Die Enteropneusten des Golfes von Neapel und der angrenzenden Meeres-Abschnitte. Monographie 18. Friedländer, Berlin. 758 pp. + Pl. I–XXVII.

——— 1902. Die Benennung der Enteropneusten-Gattungen. Zool. Jahrb. Abt. Syst. Geogr. Biol. Tiere 15: 209–218.

Thiel H 1979. Structural aspects of the deep-sea benthos. Ambio Spec. Rep. 6: 25–31.

Urata M, Iwasaki S, & Ohtsuka S 2012. Biology of the swimming acorn worm *Glandiceps hacksi* from the Seto Inland Sea of Japan. Zoolog. Sci. 29: 305–310.

Wenneck TdeL, Falkenhaug T, & Bergstad OA 2008. Strategies, methods, and technologies adopted on the RV *G*. O. Sars Mar-Eco expedition to the Mid-Atlantic Ridge in 2004. Deep-Sea Res. II 55: 6–28.

Willey A 1899. Remarks on some recent work on the Protochorda, with a condensed account of some fresh observations on the Enteropneusta. Q. J. Microsc. Sci. 42: 223–244.

Young CM, Tyler PA, Cameron JL, & Rumrill SG 1992. Seasonal breeding aggregations in low-density populations of the bathyal echinoid *Stylocidaris lineata*. Mar. Biol. 113: 603–612.